2.C Studies of Thermal Electron Transport Inhibition in Steep Temperature Gradients

Thermal conduction of energy by electrons plays a dominant role in the behavior of ablatively accelerated laser fusion targets. It is a consequence of momentum conservation that the energy transported to the ablation surface, by the electrons heated at the critical surface, results in the inward accelerations of the target. Understanding the mechanisms of the thermal conduction process is an essential ingredient in a proper description of the ablative acceleration process required to achieve efficient successful laser-driven implosions of thermonuclear targets.

The commonly used description of thermal conduction was derived by Spitzer and Harm assuming that the electron-ion collision mean-free-path is much smaller than typical temperature scale lengths. In plasmas produced by high-power lasers this assumption fails because of the short scale lengths and high temperatures encountered near the heat front, yielding in some cases calculated characteristic speeds for the thermal heat flow larger than the local electron thermal speed. To avoid non-physical behavior, the upper limit of the heat flux is often assumed to be the "free streaming" limit for an isotropic Maxwellian distribution, commonly written as $Q_f = \alpha\, n_e k T_e\, (kT_e/m_e)^{1/2}$ where $\alpha = 3\ \sqrt{3}/8 \sim 0.65$. However, the analysis of many experimental results, including both long[2,3] and short[4,5,6,7,8] wavelength lasers, suggest that α is smaller by about an order of magnitude; typically $0.03 \le \alpha \le 0.1$. The use of such a small value of α, without a physical basis, is unsatisfactory, and has led to large uncertainties in target design and the simulation of experiments.[9]

The small value of α has been attributed to a variety of anomalous processes, including magnetic fields, ion acoustic instabilities,[10] and electric fields generated by suprathermal electrons,[11] but the importance of the above processes has not yet been demonstrated. In his recent review of ion acoustic turbulence models, Mead[12] has shown that the fluctuation levels required to reduce the flux limiter to the small values needed to model experiments are much too large to be plausible. An alternative explanation for the inhibition of thermal electron transport has been that the Spitzer-Harm (S-H) description should not be applied to steep temperature gradients, and that a correct treatment of classical conduction based on classical Coulomb collisions would result in lower values for the thermal conductivity than previously suggested. Recent numerical solutions[13,14] to the full Fokker-Planck equation indicate a reduction of the thermal heat flux in steep temperature gradients by roughly an order of magnitude from that given by the S-H description. The incorporation of a Fokker-Planck treatment for thermal electron transport in laser fusion simulation codes would be prohibitive, and therefore an approximate treatment, such as will be discussed in this work, is desirable.

The failure of the S-H theory to predict the heat flow in steep temperature gradients arises primarily for the following two reasons:

a. The particle flux in the S-H formalism is not bounded by the upper limit required by the transport equation, resulting in unphysically large particle and heat fluxes in the case of steep gradients.

b. Non-local effects, where long mean-free-path electrons deposit their energy ahead of the thermal region, cause modifications to the temperature profile, including some preheating.

In Subsection I we shall discuss the first effect, which is local in nature, and present a simple extension to the S-H theory by imposing a physically motivated limit on the anisotropic portion of the electron distribution function, resulting in a description of the electron thermal conduction in steep temperature gradients.[15] This model accounts for most (but not all) of the reduction in the heat flux inferred from experiments, and in typical cases gives results approximately equivalent to a flux-limiter of $\alpha \simeq 0.08$. This model is extended in Subsection II to take into account the non-local effects, and as a result the effective flux limiter is reduced somewhat further, to $\alpha = 0.03$-0.05, in agreement with the value needed to explain transport and absorption experiments.

I. Local Model for Transport Limitation

We follow the derivation of the electron thermal conductivity given by Spitzer and Harm. In the presence of small gradients we assume that the distribution function $f(x,v,\mu,t)$ has a weak angular dependence and can be expressed by a diffusion description:

$$f(x,v,\mu,t) = f_0(x,v,t) + \mu f_1(x,v,t), \qquad (1)$$

where f_0 and f_1 represent the local isotropic and anisotropic components, respectively. (In more general transport descriptions f_0 and f_1 are the first two angular moments of the distribution function.) In Eq. (1), x is the spatial coordinate, v the velocity, and μ the cosine of the angle θ between the velocity vector and the x-direction. In the case of thermal equilibrium f_0 is the local Maxwellian, and f_1 can be obtained by taking the first angular moment of the Boltzmann transport equation for f. We assume steady state and charge neutrality, which is equivalent to the zero current condition given by

$$J = (4\pi e/3)\int_0^\infty v^3 \, f_1 \, dv = 0 \quad , \qquad (2)$$

yielding an expression for the self-consistent electric field. We assume Coulomb scattering: the collisional mean-free-path is then $\lambda(v) = \lambda_0 (v/v_{th})^4$, where v_{th} is the thermal velocity $(2kT/m)^{1/2}$, and λ_0 is the total mean-free-path for $90°$ scattering by multiple collisions at kT $(\lambda_0 = (kT)^2/(\pi n_e(Z+1)e^4 \, 1n \, \Lambda \,))$.[1] Using these assumptions one finds the ratio f_1/f_0 is:

$$\frac{f_1}{f_0} = \frac{\lambda_0}{L}\left(\frac{v}{v_{th}}\right)^4\left[\left(\frac{v}{v_{th}}\right)^2 - 4.0\right] \qquad (3)$$

where L is defined by $L \equiv (T/|\ dT/dx|\ )$. Finally, the net heat flux Q is defined by $Q = (4\pi m/6)\int_0^\infty v^5 f_1 dv \equiv \int_0^\infty Q(v)dv$, which upon substitution of Eq. (3), yields Fourier's law for heat conduction: $Q = -\kappa dT/dx$, where κ is the S-H electron thermal conductivity for high Z plasmas.

From Eq. (3) it can be seen that f_1/f_0 increases with λ_0/L, and at some velocity, depending on λ_0/L, it becomes greater than unity. However, the S-H diffusion description cannot be valid for $f_1 > f_0$. When f_1 exceeds f_0 the S-H formulation breaks down because the distribution function, f, becomes negative for some μ.[16] Furthermore, for any transport description the particle flux, $v\int d\mu$ $\mu f(\mu) \equiv f_1 v/3$, cannot exceed the free-streaming value $\mu_{max} f_0 v$, where μ_{max} is the maximum allowed average of μ over the distribution function. For a half-isotropic distribution streaming into a vacuum this limit is 0.25 $f_0 v$, resulting in $f_1 \leq 0.75\ f_0$. (For the exteme case of a collimated beam of particles, $f_1 = 3 f_0$.) Therefore, at those velocities for which f_1 exceeds f_0, the S-H heat flux, Q(v), becomes unphysically large,[16] independent of the assumed transport treatment.

In the present work no attempt has been made to solve the transport equation in order to obtain the actual $f_1(v)$. However, a simple extension of the S-H local description in steep temperature gradients (high λ_0/L) can be obtained by limiting $f_1(v)$ to an upper limit $f_{1,m}(v)$, before calculating the net heat flux, $Q = \int Q(v)dv$. Choosing $f_{1,m}(v)$, to be the local Maxwellian $f_0(v)$ will result in an upper limit to the S-H local heat flux.

By applying this limitation procedure before performing the integration we use the diffusion value for f_1 at all velocities at which it is applicable ($f_1 < f_0$), and use the upper bound $f_{1,m}$ only where it is required. The commonly used "free-streaming" limit is obtained by using the upper bound value for f_1 for the entire velocity range, independent of whether the diffusion result is applicable or not. As will be shown, this procedure needs to be applied only for high velocities (above ~2.2 v_{th} for large λ_0/L), and therefore one obtains a more restrictive upper bound to the heat flux than the "free-streaming" limit.

In order to carry out this limiting procedure self-consistently, we solve for $f_1(v)$ simultaneously with the neutralizing electric field. We note that using a limited f_1, without self-consistently determining the electric field, results in non-zero currents, and for $\lambda_0/L \sim 0.05$, negative net Q's.

The results of the above treatment are compared to the S-H theory in Fig. 18. Spitzer-Harm theory predicts that the bulk of the energy is carried by electrons with velocities between 2 v_{th} and 3.5 v_{th}. In Fig. 18a, $\lambda_0/L = 0.002$, where S-H theory is expected to

Fig. 18
Spitzer-Harm (dashed curves) and self-consistent flux limited (solid curves) particle flux. f_1/f_0, and heat flux, Q(v) (in relative units). for (a) $\lambda_0/L = 0.002$; and (b) $\lambda_0/L = 0.1$. The maximum absolute value of Q(v) illustrated in (a) is 0.02 of the value in (b).
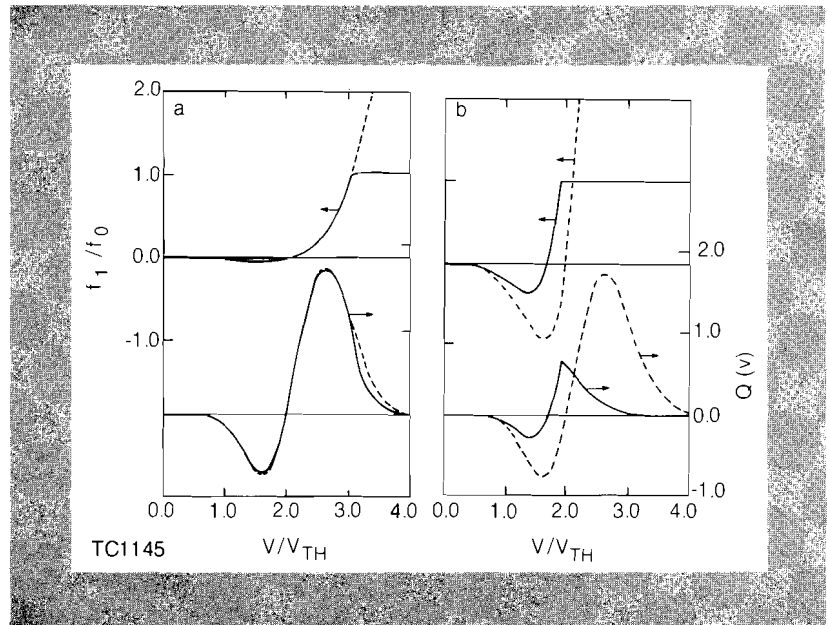
be accurate, f_1 exceeds its maximum value only at $v = 3\ v_{th}$, and since Q is insensitive to Q(v) in this range, the limiting procedure does not significantly change Q from the S-H heat flux for this small λ_0/L. In contrast, note that for $\lambda_0/L = 0.1$ (Fig. 18b), which violates the assumptions of S-H theory as illustrated by f_1 which exceeds f_0 near $v = 2\ v_{th}$, limiting f_1 sharply reduces the heat flux Q(v). Limiting the positive portion of f_1 also results in a substantial reduction in the return current needed to preserve charge neutrality, and hence a reduction in the required electrical field.

The reduction of the heat flux below the S-H value is illustrated in Fig. 19 as a function of λ_0/L. We choose Z = 4 for comparison with Ref. 13 and the e-e contribution to κ is included by using the δ_T of Ref. 1 (for Z =4, $\delta_T \sim 0.5$). The plotted range of λ_0/L extends from 10^{-4}, (where S-H theory applies), to unity, where non-local transport effects dominate. Curve I shows the reduction obtained from the self-consistent treatment when f_1 is limited to its maximum physical value f_0. *This limitation represents a new upper limit to the local S-H heat flux, which is substantially lower than the free-streaming flux (Q_f with $\alpha = 0.65$, curve II).*

To obtain the correct net heat flux as a function of λ_0/L the actual dependence of f_1 on v must be obtained. However, to estimate the reduction in the net heat flux a simple model for the transition of f_1 to its maximum value (f_{1m}) was obtained by use of a "harmonic" mean $f_{1\ell} = (f_1^{-1} + f_{1m}^{-1})^{-1}$. Curve III (Fig. 19) shows the results obtained by this method for $f_{1m} = 0.75 f_0$, which corresponds to a half-isotropic distribution streaming into vacuum ($\mu_{max} = 0.25$). A choice of f_{1m} between 0.5 f_0 and f_0 is not crucial since Q varies only by 10-25% over this range of f_{1m}. The results of this local treatment (Curve III) yield an order of magnitude reduction in the heat flux, in the range $0.03 < \lambda/L < 0.1$, which is typical of the conditions at the "top of the heat front" where the main thermal inhibition occurs (see Fig. 20 here), and can be seen to agree with
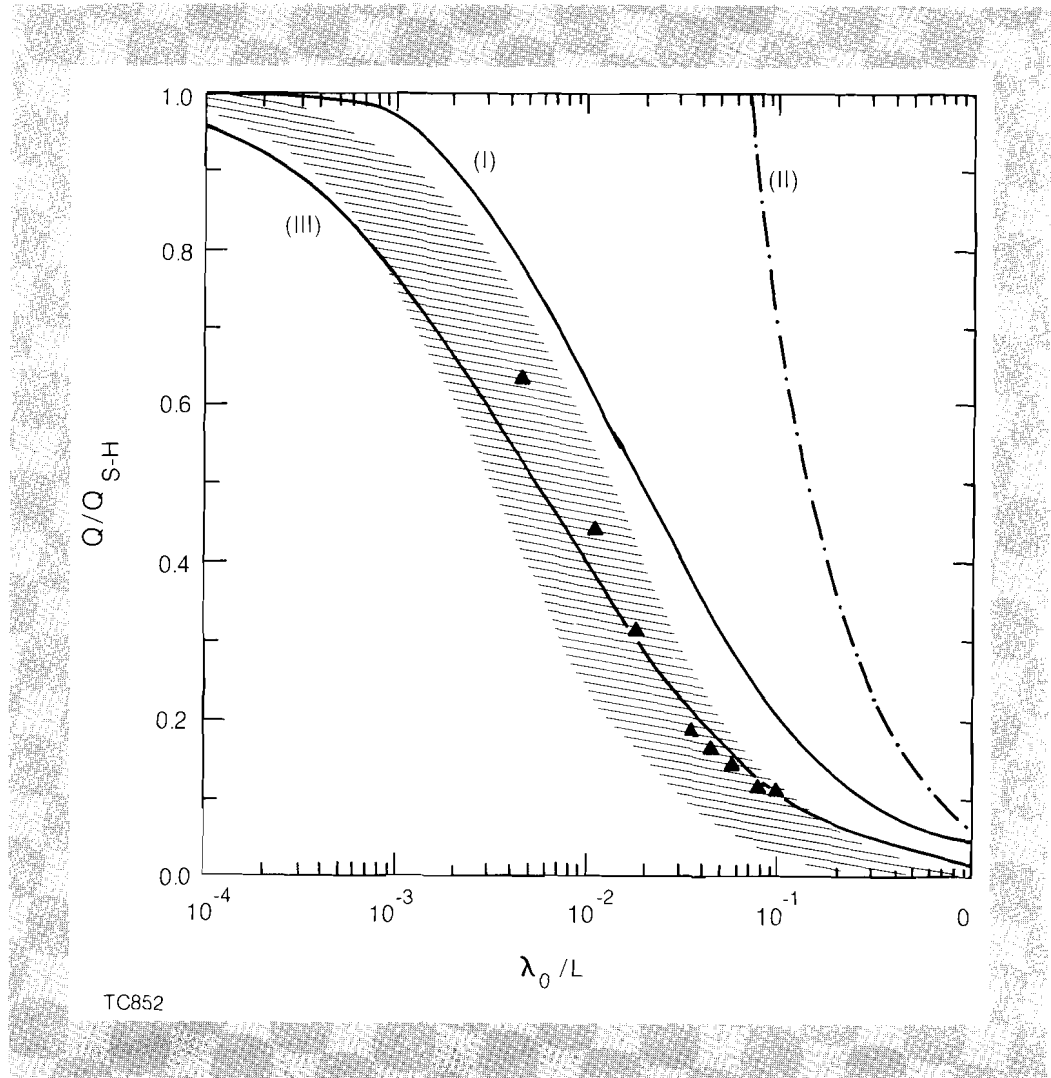
TC852

Fig. 19

Reduction of Spitzer-Harm electron thermal flux as a function of λ_0/L for Z = 4:

I. *Self consistent limitation ($f_1 < f_0$) with a sharp cut-off (see Fig. 19);*

II. *Free streaming net flux limitation ($\alpha = 0.65$) with a sharp cut-off;*

III. *Same as I with $f_1 < 0.75\, f_0$ with a "harmonic" cut-off.*

The shaded region is bounded by $0.03 < \alpha < 0.1$ using a "harmonic" cut-off. Triangles from Ref. 13: note that the λ_0 of Ref. 13 is a factor of 2.25 higher than that defined here.

the results from Ref. 13. Note that in this region of λ_0/L, the mean free path, λ, of the electrons carrying most of the energy (for $V \sim 2v_{th}$, $\lambda \cong 16\lambda_0$) is approximately equal to the temperature gradient scale length L supporting our premise that the heat flux there is predominantly local. (One might anticipate this result by analogy with the results for the minimum thickness for a strong shock[14].) Our local treatment cannot be applied to predict the preheating at the "base of the front" where nonlocal contributions dominate, due to nearly collisionless electrons streaming from the heated region. The shaded area in Fig. 19 indicates the "inhibition" obtained for $0.03 < \alpha < 0.1$ from using a "harmonic" mean heat flux as in Eqs. (1) and (2), and encompases both Curve III and the results of Ref. 13 (the triangles in the figure). From Fig. 19 we can conclude that the equivalent flux-limiter, α, needed to fit Curve III varies from about 0.05 at $\lambda_0/L \sim 0.01$ to 0.1 at $\lambda_0/L \sim 0.1$, corresponding to respectively lower and higher intensities.

The reduction in the S-H thermal conductivity derived from the new formulation (Curve III in Fig 19) has been introduced into the

hydro-code LILAC. Fig. 20 compares the temperature profile obtained by using the new model with those obtained using the harmonic flux limiter method in the range $0.03 \leq \alpha \leq 0.1$. Both absorption and penetration depth results with the new model are
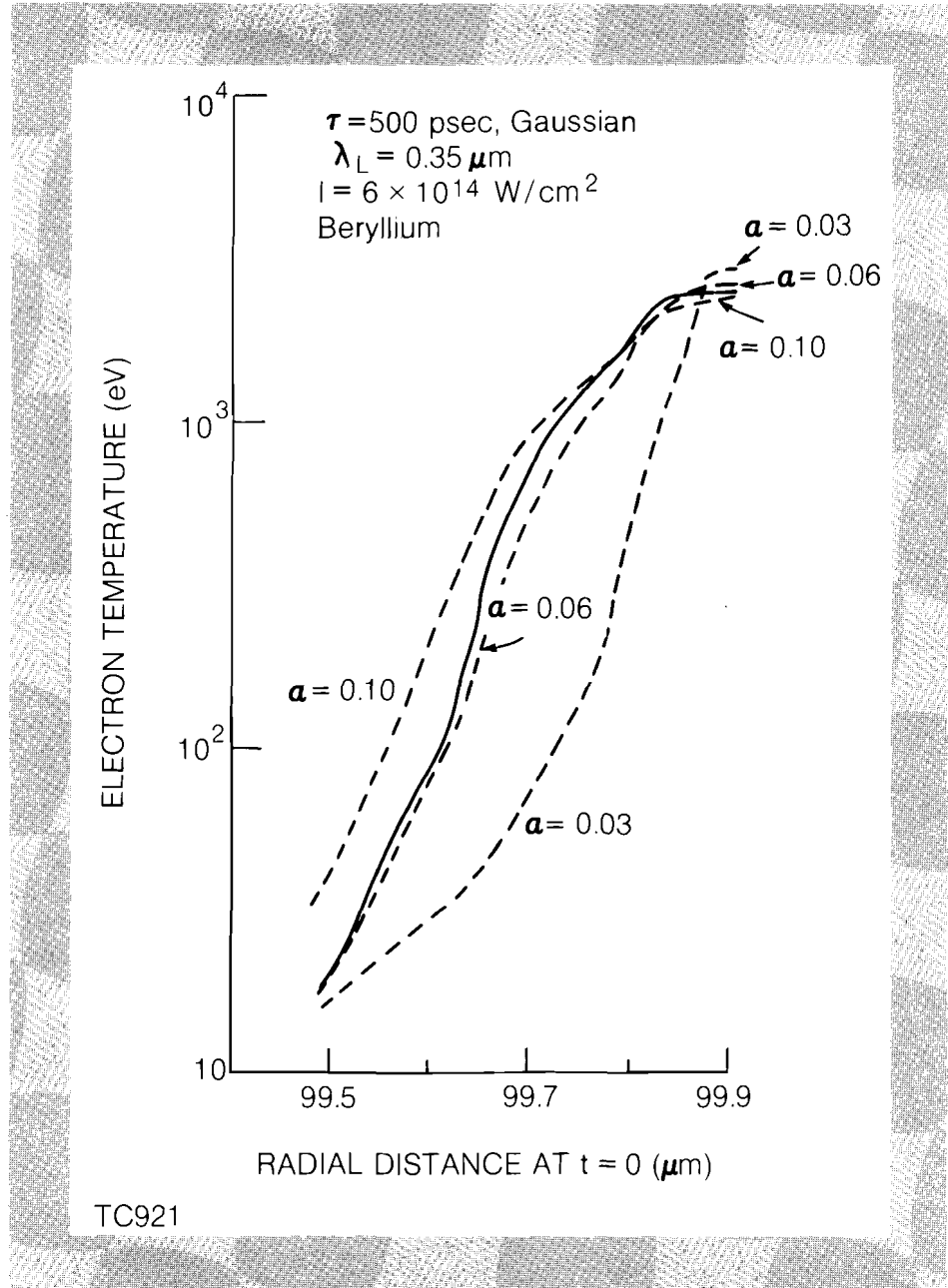

$\tau =500$ psec, Gaussian
$\lambda_L = 0.35\,\mu m$
$I = 6 \times 10^{14}$ W/cm^2
Beryllium

TC921

Fig. 20
Temperature profiles in the heat front, plotted at the peak of the pulse against the (initial) Lagrangian coordinate, for the self-consistent local model (solid line) and for the flux-limiter model with various values of f (dashed lines). The target is beryllium, and the laser parameters are: $\lambda_L = 0.35\,\mu m$, $\tau = 500$ psec, $I = 6 \times 10^{14}$ W/cm².

similar to those obtained with $\alpha \sim 0.06$-0.1. Figure 21 shows the temperature profile at the heat front, obtained with the new formulation, along with the ratio λ_0/L. This ratio peaks at the top of the heat front with a value 0.04, thus confirming the assumption that $\lambda_0/L < 0.1$ at the heat front. The general structure of the heat front illustrated Figs. 20 and 21 is typical of a wide range of laser irradiance conditions and target compositions.
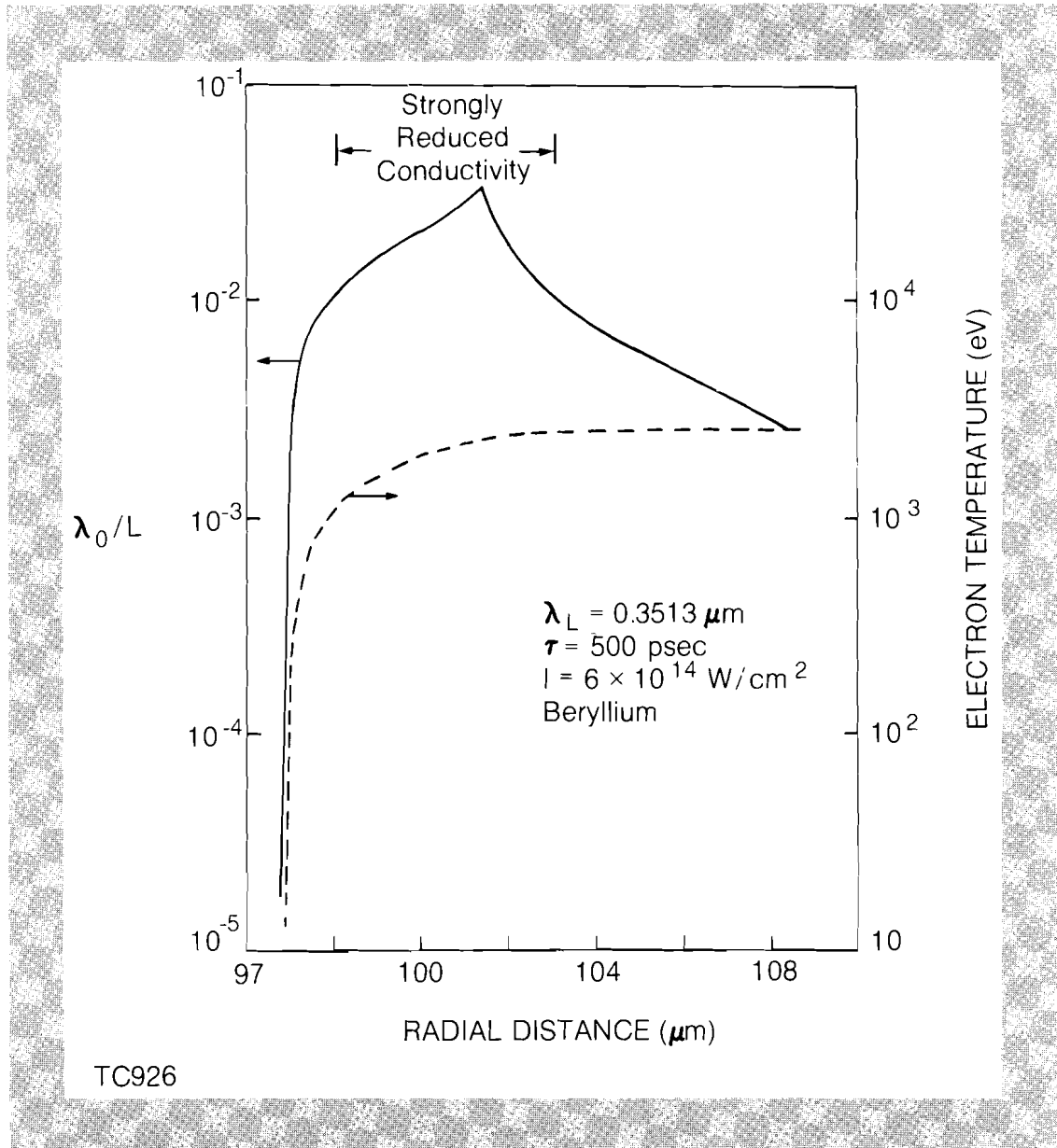
25

TC926

Fig. 21
Profiles of λ_0/L (solid line) and electron
temperature (dashed line) calculated
by LILAC for the conditions of Fig. 20.

Figure 22 compares the maximum value of λ_0/L obtained at various irradiation intensities from LILAC simulations using the self consistent formulation with those using a flux limiter of 0.03 and 0.06. The curve for a = 0.03 is very close to the corresponding curve in Fig. 5 calculated by SAGE. It is seen that the values of λ_0/L obtained using the self-consistent local model are slightly below those obtained with $\alpha \sim 0.06$ and far below those obtained using $\alpha \sim 0.03$. This result is consistent with the observation made from Figs. 15 and 16 above that the effective flux-limiter ranges from 0.06-0.1 depending on the laser intensity.
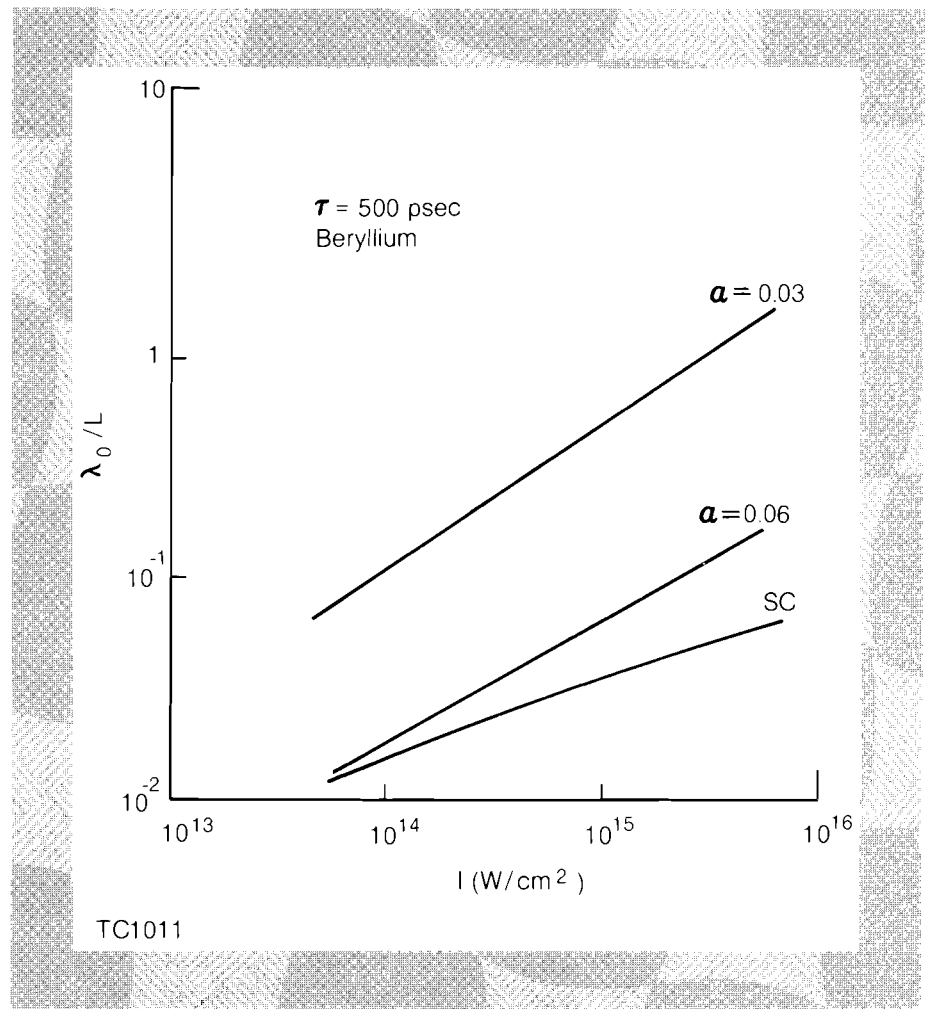
Fig. 22
Dependence of the maximum λ_0/L on laser intensity, for the self-consistent local model and for the flux-limiter model.

II. Hybrid Model for Non-Local Thermal Transport

We expect the model described above to be applicable for gradients of $\lambda_0/L < 0.1$, where the transport is mainly local in nature. This should be the case in steady heat flow situations, where energy is supplied at the edge of a plasma, and a thermal front propagates into the plasma with its temperature profile adjusting to give $\lambda_0/L < 0.1$. Thus, it is not surprising that the results of our local model and the Fokker-Planck treatment of Ref. 13 are in close agreement.

However, in typical laser-plasma interaction experiments, the laser energy is deposited predominantly in the leading edge of the heat front, causing the temperature gradient there to steepen and give values of λ_0/L in excess of 0.1. Significant non-local energy transport and deposition then takes place, due to the nearly collisionless electrons, resulting in a broadening of the temperature profile at the base of the front and also some preheating. The amount of energy deposited within the characteristic gradient length of the front is reduced, implying a further reduction in the main thermal bulk penetration depth.

27

In order to account for these non-local contributions, a hybrid model was developed. Here the electrons are treated as a single fluid, except that the energy transport is performed by a multi-group flux-limited diffusion treatment[18] for electrons above some velocity v^*. This velocity is chosen to be the velocity at which the integrated heat flux ($_0\int^{v^*} Q(v)dv$) is zero, based on the self-consistent local treatment. For the entire range of λ_0/L this v^* lies in the range 2-2.5 v_{th}. From the self-consistent local treatment at velocities up to v^*, $f_1 < f_0$, confirming the assumed local treatment there, and explaining the lack of sensitivity of v^* to the exact form of f_1/f_0 in the flux limited region.

We have compared the hybrid model with a full Fokker-Planck calculation,[19] using a test case similar to that of Ref. 19 where the plasma is heated at one end to a constant temperature. The initial temperature and density profiles are shown in Fig 23 (dotted lines). The temperature in the underdense region ($n_e \cong 10^{21}$ cm^{-3} in this example) is maintained at 1.1 keV throughout. Results are shown for the temperature profiles after 150 psec, as calculated by the hybrid model (dashed line) and the flux-limiter model (solid lines) for $\alpha = 0.05$-0.2. The hybrid result is well approximated by the result for $\alpha = 0.1$, in agreement with the conclusion of Refs. 13 and 19. In this case the contributions of the electrons transported non-locally by the multigroup treatment were relatively small, as expected.

Fig. 23
Initial temperature and density profiles for a transport test problem (dotted lines), and the resulting temperature profiles after 150 psec calculated by the hybrid model (dashed line) and the flux-limiter model (solid lines). The spatial coordinate is Lagrangian.

TC1061 RELATIVE INITIAL DISTANCE (μm)
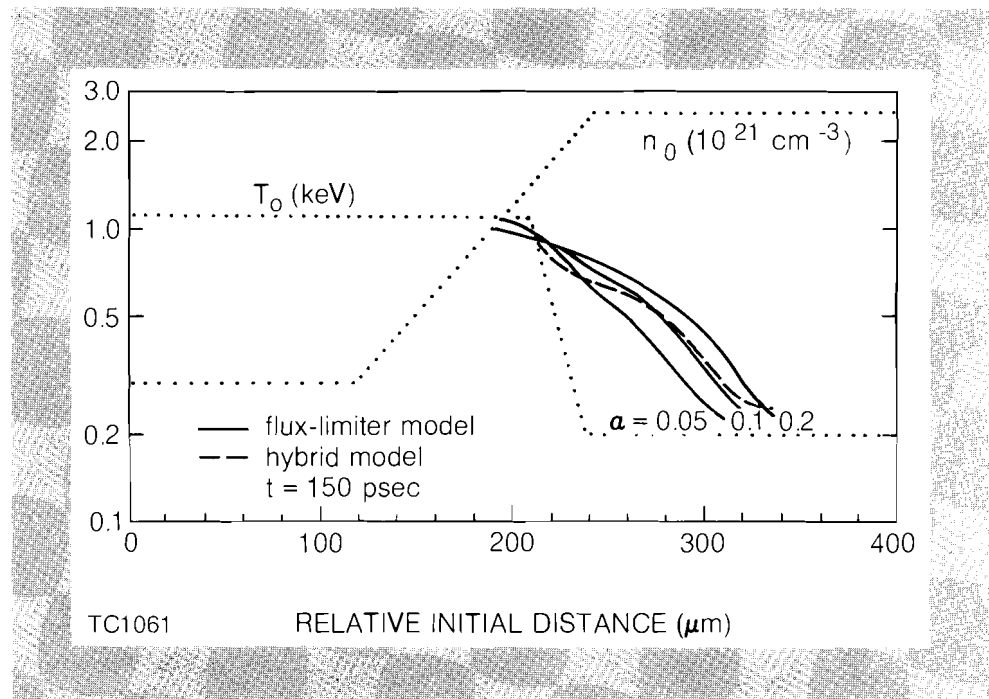
The non-local contributions should however be important under the more general conditions of laser-target interactions. Calculations of absorption and transport, under conditions typical of the 0.35 μm experiments carried out recently at LLE[7,8] (for 400-500 psec pulse widths), are shown in Fig. 24, for the hybrid model and for the flux-limiter model with $\alpha = 0.03$ and 0.06.

- $\lambda = 0.3513 \ \mu m$, $\tau = 500$ psec
- IB absorption only
- Penetration depth: 500 eV position at peak of pulse
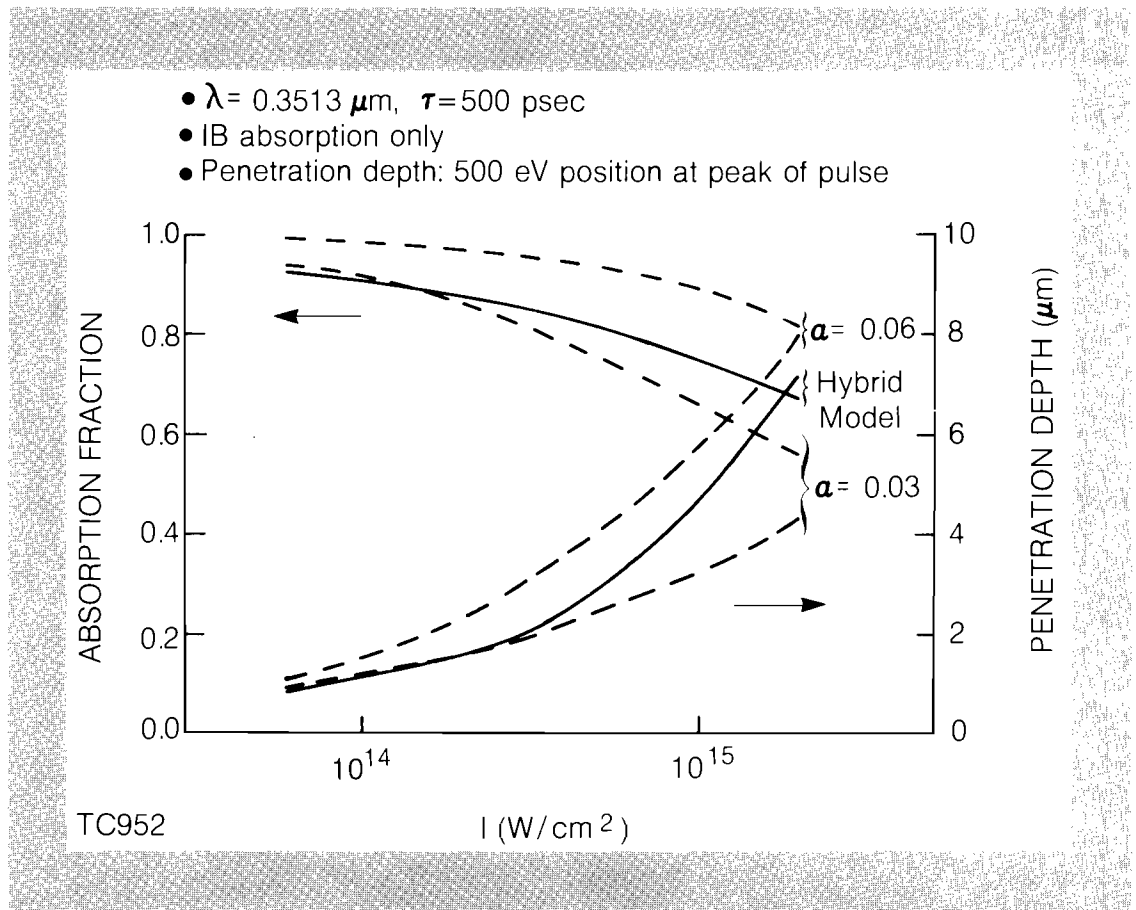
TC952   I (W/cm^2)

Fig. 24
Calculated absorption fraction and penetration depth as a function of laser intensity, for the non-local hybrid model (solid lines) and for the flux-limiter model (dashed lines). Targets are CH, and the laser parameters are $\lambda_L = 0.35 \ \mu m$ and $\tau = 500$ psec.

No fast electron dump was included in any of these simulations. It is notable that the predictions of the hybrid model, like the experimental results[7,8,] lie within the flux-limiter model predictions for $\alpha = 0.03$-0.06; in both cases the agreement is best for a value of α closer to 0.03.

In Fig. 25 the temperature profiles are given for typical irradiation conditions, and for the hybrid model and the same two values of α; the horizontal coordinate is a Lagrangian coordinate relative to the initial target position. The steep temperature gradient at the top of the heat front predicted by the hybrid model, and the smoothing of the temperature profile at the base of the front as discussed above, are clearly seen. The penetration depth, defined here by the excursion of the 500 eV contour at the peak of the pulse, lies between the $\alpha = 0.03$ and $\alpha = 0.06$ predictions in accordance with Fig. 24.

From Fig. 25 it is seen that the corona temperature predicted by the hybrid model is smaller than the result for $\alpha = 0.03$. This occurs because the fastest electrons are not inhibited from streaming out of the corona and into the denser cold material.

Our analysis of heat transport suggests that a distinction should be made between the reduced energy flow across the top of the heat front, which results primarily from the limitation
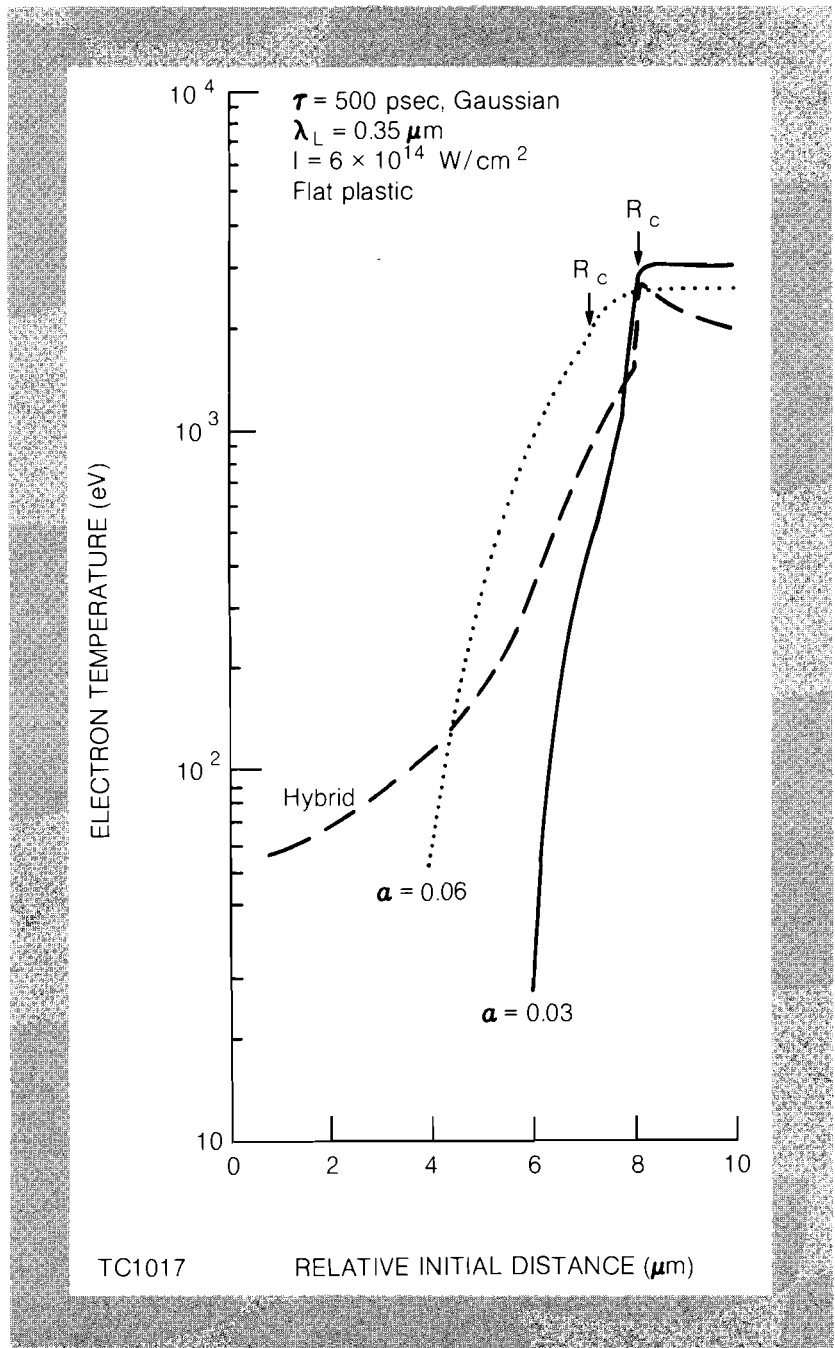
Fig. 25
Temperature profiles in the heat front,
plotted at the peak of the pulse against
the (initial) Lagrangian coordinate, for
the hybrid model (dashed line) and the
flux-limiter model with α = 0.03 and
0.06.

imposed on the perturbed distribution function, and the propagation of temperature contours (such as the 500 eV contour used here to identify the "penetration depth"), which depend on the deposition profile of this energy flow. The first process is typically described by a flux-limiter $\alpha \sim 0.08$ (see subsection I). The second effect can be estimated by calculating the fraction of energy deposited within one gradient scalelength L. We assume that this energy causes the heat front to advance, while energy deposited at distances further than L results mainly in preheating. Using simple analytic formulas of energy deposition,[23] we have calculated that less than 50% of the energy flowing across

the top of the heat front is deposited within a distance L, for $\lambda_0/L >$ 0.1. Combining both effects, we obtain an effective flux-limiter of about 0.04 for the propagation of temperature contours.

In summary, we have shown that the 'thermal inhibition" seen in steep temperature gradients, previously attributed to a variety of "anomalous processes", does not require such processes for its explanation. The need for very small flux limiters arose from the incorrect application of the S-H formula far from its regime of applicability, that is when the electrons responsible for the heat flow have mean free paths comparable or greater than the gradient scale length, and a misinterpretation of the classical free-streaming ($\alpha = 0.65$) flux limiter as representing the maximum heat flux. Accounting appropriately for these effects, we have obtained "effective flux limiters" of about 0.03 in good agreement with what has been required to interpret laser plasma interaction experiments.

REFERENCES

1. L. Spitzer and R. Harm, *Phys. Rev.* **89**, 977 (1953).

2. R. C. Malone, R. L. McCrory, and R. L. Morse, *Phys. Rev. Lett.* **34**, 721 (1975).

3. W. L. Kruer, *Comment Plasma Phys. Controlled Fusion* **5**, 69 (1979).

4. F. Amiranoff, R. Fabbro, E. Fabre, C. Garban, J. Virmont, and M. Weinfeld, *Phys. Rev. Lett.* **43**, 522 (1979).

5. D. C. Slater, G. E. Busch, G. Charatis, R. R. Johnson, F. J. Mayer, R. J. Schroeder, J. D. Simpson, D. Sullivan, J. A. Tarvin, and C. E. Thomas, *Phys. Rev. Lett.* **46**, 1199 (1981).

6. W. C. Mead, E. M. Campbell, K. G. Estabrook, R. E. Turner, W. L. Kruer, P. H. Y. Lee, B. Pruett, V. C. Rupert, K. G. Tirsell, G. L. Stradling, F. Ze, C. E. Max, and M. D. Rosen, *Lawrence Livermore National Laboratory Report* **UCRL-84684** (1981).

7. W. Seka, R. S. Craxton, J. Delettrez, L. M. Goldman, R. Keck, R. L. McCrory, D. Shvarts, J. M. Soures, and R. Boni, submitted for publication.

8. B. Yaakobi, T. Boehly, P. Bourke, Y. Conturie, R. S. Craxton, J. Delettrez, J. M. Forsyth, R. D. Frankel, L. M. Goldman, R. L. McCrory, M. C. Richardson, W. Seka, D. Shvarts and J. M. Soures, to be published in Optics Comm.

9. C. E. Max, C. F. McKee, and W. C. Mead, *Phys. Fluids,* **23**, 1620 (1980).

10. W. M. Manheimer, *Phys. Fluids,* **20**, 265 (1977).

11. I. P. Shkarofsky, *Phys. Rev. Lett.* **42**, 1342 (1979).

12. W. C. Mead, *Lawrence Livermore National Laboratory Report,* **UCRL-85246** (1980).

13. A. R. Bell, R. G. Evans, and D. J. Nicholas, *Phys. Rev. Lett.* **46**, 243 (1981).

14. R. J. Mason, *Bull, Am. Phys. Soc.* **25,** 926 (1980); R. J. Mason, *Los Alamos National Laboratory Report* **LA-UR-81-95** (1981).

15. D. Shvarts, J. Delettrez, R. L. McCrory, and C. P. Verdon, *Phys. Rev. Lett,* **47,** 247 (1981).

16. D. R. Gray and J. D. Kilkenny, *Plasma Phys.* **22,** 81 (1980).

17. Ya. B. Zel'dovich and Yu. P. Raizer, *Physics of Shock Waves and High-Temperature Hydrodynamic Phenomena,* (Academic Press, New York, 1966), vol. **1,** chap. 1, p. 84.

18. D. Shvarts, C. Jablon, I. B. Bernstein, J. Virmont, and P. Mora, *Nuc. Fusion* **19,** 1457 (1979).

19. A. R. Bell, Paper 6-1, *11th Annual Anomalous Absorption Conference, Montreal* (1981).

20. M. D. Rosen, *Lawrence Livermore National Laboratory Annual Report* **URCL-50021-79,** p. 3-6 (1979).